ASSOCIAZIONE NAZIONALE ITALIANA DI INGEGNERIA SISMICA ANIDIS
Italian National Association of Earthquake Engineering
XVIII CONVEGNO ANIDIS
L'ingegneria sismica in Italia
ASCOLI PICENO 2019
15-19 Settembre

Exterior RC beam-column joints: experimental outcomes and modeling issues

Riccardo Nitiffi[a], Ernesto Grande[b], Maura Imbimbo[a], Annalisa Napoli[c], Roberto Realfonzo[c]
[a]*Department of Civil and Mechanical Engineering. University of Cassino and Southern Lazio. Via G. Di Biasio 43, 03043, Cassino (FR).*
[b]*Department of Sustainability Engineering. University Guglielmo Marconi. Via Plinio 44, 00193,Roma.*
[c]*Department of Civil Engineering. University of Salerno. Via Giovanni Paolo II 132, 84084, Fisciano (SA).*

Keywords:RC beam-column joints; experimental tests; numerical analyses.

ABSTRACT
The attention of the scientific community toward the evaluation of the seismic safety of existing RC buildings is testified by the amount of studies available in the current literature and, also, by the frequent updates of national codes. Indeed, the extended damages and collapses exhibited by RC buildings during the last decades earthquakes, highlighted the need of better understanding the influence of structural details on the seismic response in order to improve guidelines and, at the same time, to carry out efficient strengthening techniques for existing buildings. In this context, the beam-column joint assumes a relevant role since it could particularly affect the seismic vulnerability of RC buildings. The present paper is part of a research activity involving different universities, aimed at investigating the behavior of RC beam-column joints of buildings designed in agreement with past Italian codes and, in particular, the efficacy of strengthening interventions based on the use of innovative composite materials. The paper presents the experimental and numerical results carried out with reference to an unstrengthened joint, designed with the aim to simulate the behavior of an exterior joint. After the introduction, reporting a brief state of art, a description of the main outcomes emerged from the experimental tests and numerical analyses are presented in detail.

1 INTRODUCTION

The significant damages occurred in existing RC buildings during the past and recent earthquakes have underlined the key role of the beam-column joints in the seismic response of these systems and their remarkable vulnerability in case of exterior configurations and poor steel reinforcement details.

This has led the scientific community to better investigate the response of the beam-column joints and, also, to introduce into the codes more detailed recommendations for their design and analysis. The Italian guidelines (NTC08 2008 and NTC18 2018) represent a recent example.

Some studies available in literature (Realfonzo et al. 2014; Del Vecchio et al. 2014; De Risi et al. 2016) mainly aim at investigating the experimental behavior of RC beam-column joints belonged to existing buildings and designed in agreement with past codes which did not contain any specific recommendations for these structural components. Other studies focus the attention on analysing the efficacy of strengthening interventions by using composite materials (Akguzel and Pampanin 2012; Realfonzo et al. 2014; Napoli et al. 2016; De Vita et al. 2017).

Moreover, a number of studies developed numerical models able to simulate the kinematics of beam-column joints and the main phenomena characterizing their nonlinear response (Vecchio and Collins 1986; Alath and Kunnath 1995; Biddah and Ghobarah 1999; Lowes and Altoontash 2003; Shafaei et al. 2013).

The study presented in this paper deals with the modelling of the cyclic response of RC beam-column joints. To this purpose, several models from the technical literature are considered in order to simulate the behavior of exterior joints tested at the University of Salerno (Realfonzo et al. 2014; De Vita et al. 2017). The comparison between the experimental and the numerical results provides some preliminary considerations on the accuracy of the examined models in the assessment of the joint seismic behavior.

2 RC JOINT MODELING

The introduction of rigid links simulating the panel zone is one of the approaches widely used in literature despite the criticisms related to its inability to account for the contribution of the shear deformation affecting the panel zone (Shafaei et al. 2013). For this reason, some authors (Alath and Kunnath 1995; Biddah and Ghobarah 1999; Lowes and Altoontash 2003) proposed “multi-spring models” in which the rigid links are coupled with rotational nonlinear springs able to better reproduce the experimental beam-column joints behavior.

Among the multi-spring models, Biddah and Ghobarah (1999) proposed an approach based on the use of two different nonlinear rotational springs to simulate the shear behavior and bond-slip phenomena (Figure 1a); here the cyclic response of the joint is schematized throughout a tri-linear idealized hysteretic relationship without accounting for the pinching effect.

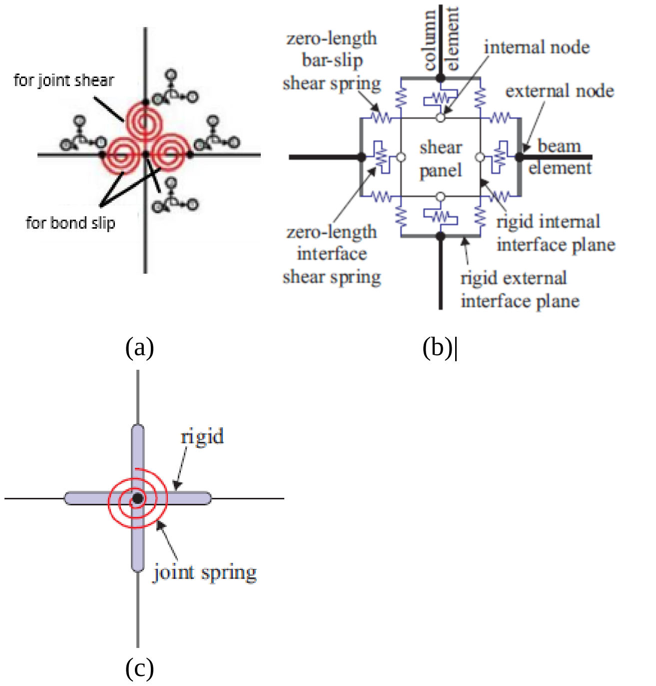

Figure 1. Biddah and Ghobarah (1999) multi-spring model (a); Lowes and Altoontash (2003) multi-spring model (b); Alath and Kunnath (1995) scissors model (c).

Another contribution is given by Lowes and Altoontash (2003); in this paper the authors proposed a 4-node 12-degree-of-freedom macro-model element (Figure 1b) with eight zero-length translational bar slip springs, four interface shear springs, and a panel zone whose shear stress-strain relationship curve is defined through the MCFT approach (Vecchio and Collins 1986). This model allows to account for the pinching effect and it was further improved by Altoontash (2004) and Mitra and Lowes (2007).

Another model, simpler than the previous ones and called “scissors model”, was proposed by Alath and Kunnath (1995). This model schematizes the joint by a master node and a duplicated slave node located at the same position in the middle of the panel zone. These nodes are connected to the beam and column members by means of rigid links (Figure 1c). Moreover, a rotational spring is introduced for connecting the master and the slave nodes. This spring, which allows only relative rotations between the connected nodes, is characterized by a constitutive law τ-γ reproducing the shear behavior of the joint.

Generally, most of the authors employing the *scissors model* introduce a multilinear law for the τ-γ relationship (Figure 2). This relationship allows to take into account the main phases characterizing the shear behavior of the joint: cracking, pre-peak, peak and residual strength (De Risi et al. 2015).

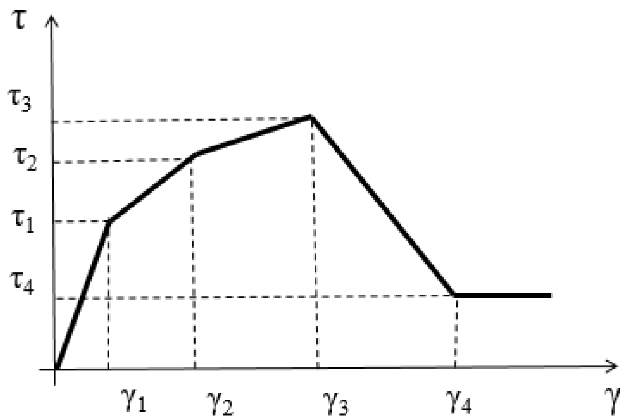

Figure 2. Multilinear stress-strain relationship for the rotational spring in the scissors model.

The values of the parameters characterizing the multilinear law (i.e.: τ_1, τ_2, τ_3, τ_4 and γ_1, γ_2, γ_3, γ_4) are generally estimated from analytical formulas or directly derived by the authors through calibration procedures based on experimental data.

In practice, the τ-γ relationship is used to reproduce the skeleton moment-rotation (M-θ) curve. Then, loading and unloading cyclic laws are associated to the skeleton curve in order to reproduce the cyclic behavior of the rotational spring and modelling the strength and stiffness cyclic degradation and the pinching phenomenon, typical of RC members.

By focusing on the law depicted in Figure 2, several authors proposed analytical formulas for the estimate of the shear strength τ_3 (= τ_{max}).

Kim and LaFave (2008) proposed:

$$\tau_{max} = \alpha_t \beta_t \eta_t \lambda_t (JI)^{0.15} (BI)^{0.3} (f_c)^{0.75} (\mathrm{MPa}) \qquad (1)$$

where:

α_t assumes a different value for exterior (=0.7) or interior (=1.0) joints;
β_t depends on the degree of exterior joint's confinement (= 1.0 for joints with no more than one transverse beam; = 1.18 for joints with two transverse beams);
η_t depends on the beam-column eccentricity (=1.0 if there is no eccentricity);
λ_t is a coefficient assumed by the authors equal to 1.31;
f_c is the concrete compressive strength;
JI is the "joint transverse reinforcement index" given by $JI=\rho_j \times f_{yj}/f_c$, where ρ_j is the geometrical percentage of the joint transversal reinforcement and f_{yj} is the yield strength of joint transverse reinforcement;
BI is the "beam reinforcement index" given by $BI=\rho_b \times f_{yb}/f_c$, where ρ_b is the geometrical percentage of the longitudinal beam reinforcement and f_{yb} is the yield strength of the reinforcement.
In the case of joints without stirrups, Vollum and Newman (1999) proposed:

$$\tau_{max} = 0.642\,\beta\left[1+0.555\left(2-\frac{h_b}{h_c}\right)\right] b_e h_c \sqrt{f_c}\ \text{(MPa)} \quad (2)$$

where:
β depends on the bending shape of the beam's longitudinal steel bar end inside the joint (= 1.0 in the case of a "L-shape" configuration; = 0.9 in the case of a "U-shape" one);
h_b is the beam height;
h_c is the column height;
b_e is the dimension of the effective joint width.
In the case of exterior beam-column joints, by using a strut and tie model, Ortiz (1993) proposed:

$$\tau_{max} = \frac{\sigma_d b_c w_j \cos\theta}{b_c b_b}\ \text{(MPa)} \quad (3)$$

where:
σ_d is the design compressive concrete strength estimated according to the CEB-fip Model Code 90 (1990);
b_c is the column width;
b_b is the beam width;
w_j is the strut width;
θ is the angle between the strut and the longitudinal beam axis.
The formula proposed by Hwang & Lee (1999) derived on the so-called "softened strut and tie mechanism" and provides:

$$\tau_{max} = \frac{D\cos\theta + F_h + F_v\cot\theta}{b_c b_b}\ \text{(MPa)} \quad (4)$$

where:
D is the compressive strength of the concrete strut component;
F_h and F_v are the horizontal and the vertical components of the strength of the tie member respectively.
Jeon (2013) modified Kim and LaFave (2008) model and provides:

$$\tau_{max} = 0.586(TB)^{0.774}(BI)^{0.495}(JP)^{1.25}(f_c)^{0.941}\ \text{(MPa)} \quad (5)$$

where:
TB coincides with β_t of Eq. (1) except for the case of joints with two transverse beams where the value changes from 1.18 to 1.2;
JP coincides with α_t of Eq (1) except for the case of exterior joints where the values changes from 0.70 to 0.75.
Further analytical models available in literature provide the others three values of the shear stress (i.e. τ_1, τ_2, τ_4).
For what concern the shear stress τ_1, most studies suggest to evaluate it throughout the formula proposed in Uzumeri (1977), that is:

$$\tau_1 = 0.29\sqrt{f_c}\sqrt{1+0.29\frac{P}{A_j}} \quad \text{(MPa)} \quad (6)$$

where *P* is the column axial load and A_j is the effective joint area.
Finally, the values of τ_2 and τ_4 are provided by De Risi et al. (2016), Celik and Ellingwood (2008), Shin and LaFave (2004) and Sharma et al. (2011) as a fraction of the maximum shear strength, τ_{max} (see Table 1).
The same authors also provide the four values of the shear strain γ_i (i.e. γ_1, γ_2, γ_3, γ_4) corresponding to the above mentioned τ_i (see Table 2).

Table 1. Values of τ_2 and τ_4

	τ_2	τ_4
De Risi et al. (2016)	0.85 τ_{max}	0.65 τ_{max}
Celik & Ellingwood (2008)	0.75 τ_{max}	0.16 ÷ 0.3 τ_{max}
Shin & LaFave (2004)	0.9 τ_{max}	0.7 ÷ 0.9 τ_{max}
Sharma et al. (2011)	1.0 τ_{max}	0.24 τ_{max}

Table 2. Shear strain values

	γ_1	γ_2	γ_3	γ_4
De Risi et al. (2016)	0.0004	0.0017	0.0049	0.0441
Celik & Ellingwood (2008)	0.0001 ÷ 0.0013	0.002 ÷ 0.01	0.01 ÷ 0.03	0.03 ÷ 0.1
Shin & LaFave (2004)	0.0005	0.002 ÷ 0.01	0.01 ÷ 0.03	0.03 ÷ 0.05
Sharma et al. (2011)	0.0006	0.002	0.005	0.025

3 EXPERIMENTAL ACTIVITY

The results presented in this paper referred to an experimental activity recently performed at the University of Salerno (Italy). The tests were carried out with reference to different configurations of RC beam-column joints (unconfined and confined joints) and also considering strengthening configurations based on the use of composite materials (Realfonzo et al. 2014; Napoli et al. 2016).

The analyses discussed in the present paper refers only to the case of the exterior unstrengthened beam-column joint denoted *J05* in Realfonzo et al. (2014).

Figure 3 shows the geometric configuration of the case study specimen; it consists of 2000 mm long columns with 300 mm × 300 mm square section, and 1700 mm long beams having a 300 mm × 400 mm rectangular section.

The longitudinal reinforcement of the column is made up of (4+4)Φ14 steel rebars, whereas the beam reinforcement is (4+4)Φ20; both members are equipped with 8 mm diameter steel stirrups, 100 mm spaced.

The amount of the steel reinforcement was designed with the purpose to simulate the case of the strong columns – weak beams failure mode. Nevertheless, due to the absence of transverse reinforcements, the joint panel was expected to fail first.

The test set-up realized to subject the *J05* joint to the experimental activity is shown in Figure 4.

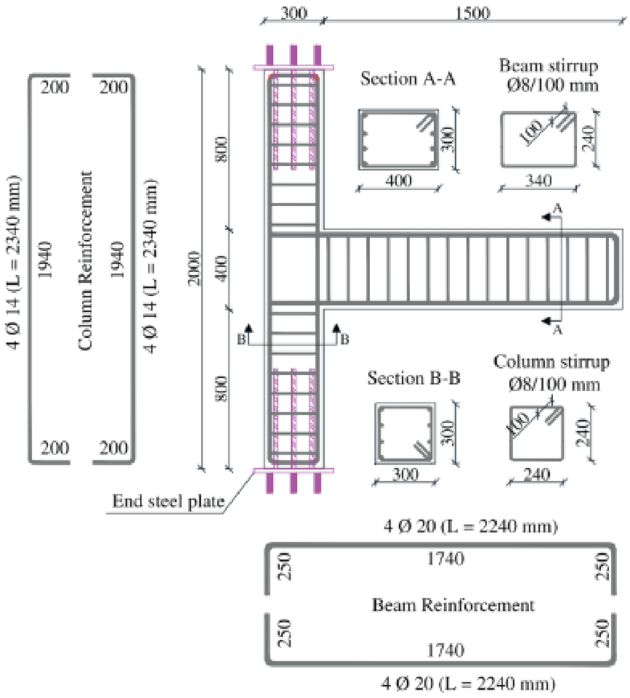

Figure 3. Geometric configuration and details for specimen J05 (Realfonzo et al. 2014).

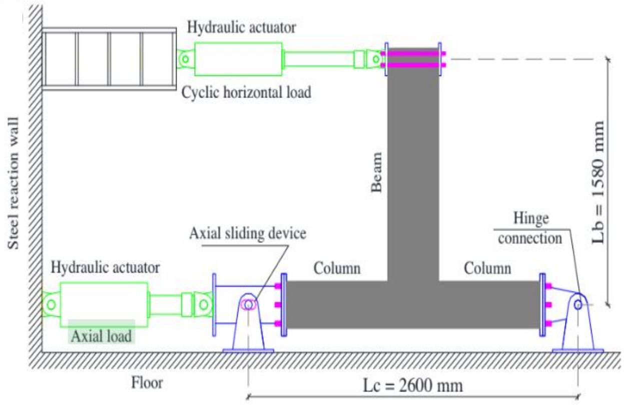

Figure 4. Test set-up configuration (Realfonzo et al. 2014).

The column was restrained to both its ends by means of steel elements simulating a roller-hinged scheme. The axial load N applied to the column was equal to about 300 kN.

A horizontal force was cyclically applied at the beam tip in displacement control through a hydraulic actuator. The imposed displacement was increased every three cycles with two different rates: 0.2 mm/s before the beam yield displacement (14 mm) and 1 mm/s after it.

With reference to the specimen *J05*, its experimental response mainly underlined the development of first cracks at the beam-column interface, whose width didn't increase during the test (Realfonzo et al. 2014; Milanese 2017). In addition, it was also observed that these cracks did not affect the overall resistance of the specimen, because the failure mode was characterized by the detachment of the external concrete wedge after the development of main cracks under the panel zone (see Figures 5 and 6).

Figure 5. Diagonal cracks of the panel zone of the specimen J05 (Realfonzo et al. 2014).

Figure 6. Detachment of the concrete cover of the specimen J05 (Realfonzo et al. 2014).

The experimental Force-Displacement response of the specimen *J05* is presented in Figure 7.

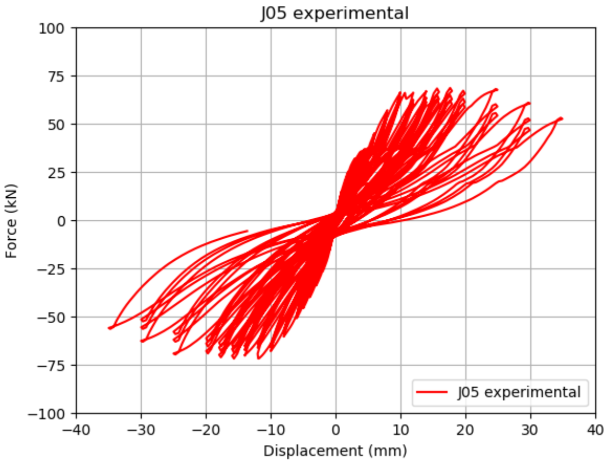

Figure 7. Specimen J05: experimental cyclic response.

4 NUMERICAL ANALYSES

The numerical analyses presented in this paper are carried out with reference to the specimen *J05*. The main goal of these analyses is to assess the capability of the literature models in reproducing the monotonic and the cyclic experimental behavior of the specimen *J05*.
Moreover, additional numerical analyses are also developed to investigate the influence of the variability of the concrete strength on the response of the joint.

4.1 Beam-column joint model

A 2D-model for the joint *J05* is here implemented by using the software OpenSees (McKenna et al. 2010). In particular, the fibre-modelling approach is used for the beam and column members, while the *scissors model* (Alath and Kunnath 1995) is employed for the beam-column joint.
For what concerns the *scissors model*, a zero-length rotational spring is introduced at the centre of the panel zone and rigid elements are considered at its edges to reproduce the connection with beam and column elements.
The dimensions of the rigid links are herein assumed equal to the semi-length of the panel zone. Moreover, no additional springs for reproducing bond-slip deformations are introduced.
An important feature of the numerical model used herein is represented by the constitutive laws at the level of materials and elements. In particular, for the beam and column members, the nonlinear uniaxial materials "*concrete04* – Popovics model" and "*steel02* – Giuffrè-Menegotto-Pinto model", available in the OpenSees library, are used for modelling the concrete and steel materials; the mechanical parameters are mainly deduced on the basis of the mechanical properties of the materials characterizing the specimen *J05* tested in the experimental campaign.
Regarding the beam-column joint element, the *pinching4 uniaxial material* is used for modelling the rotational spring. In particular, a multilinear law in terms of moment-rotation (M-θ) is assigned to the *pinching4* material, in order to schematize the shear behavior of the joint.
The M-θ curve is directly derived from the τ-γ relationship shown in Figure 2.
In fact, it is easy to demonstrate that the bending moment M_j transferred by the rotational spring can be evaluated as follows:

$$M_j = \tau_j A \frac{1}{\frac{1-h_c/2L_b}{jd_b} - \frac{1}{2L_c}} \tag{7}$$

where:
τ_j is the shear stress of the multilinear law;
A is the joint cross-section area;
h_c is the column height:
L_b is the beam length;
jd_b is the beam internal lever arm;
L_c is the column length.
On the other hand, the rotation of the spring θ_j can be assumed equal to the joint panel strain γ_j.
The *τ-γ* laws here accounted for developing the numerical analyses are obtained by combining the models of literature already discussed in detail in the introduction. In particular, each of the models providing analytical formulas for the derivation of τ_{max} is combined with each of the models providing indications about the other parameters. Moreover, for the models where the authors proposed a range of values, both the minimum and the maximum of the range are considered. Then, from the combination of the accounted literature models, a set of 30 τ-γ laws are obtained and herein used for performing preliminary analyses (see Table 3).

Table 3. Combinations of the literature models for deriving the multilinear shear stress-strain law.

	A	B*	B**	C*	C**	D
1. Kim & LaFave, 2008	1-A	1-B1	1-B2	1-C1	1-C2	1-D
2. Vollum & Newman (1999)	2-A	2-B1	2-B2	2-C1	2-C2	2-D
3. Ortiz (1993)	3-A	3-B1	3-B2	3-C1	3-C2	3-D
4. Hwang & Lee (1999)	4-A	4-B1	4-B2	4-C1	4-C2	4-D
5. Jeon (2013)	5-A	5-B1	5-B2	5-C1	5-C2	5-D

(A) De Risi et al. (2016); (B) Celik and Ellingwood (2008); (C) Shin and LaFave (2004); (D) Sharma et al. (2011)
* min values of the range; ** max value of the range

The values of shear stresses and shear strains corresponding to each of the considered models are reported in Tables from 4 to 6.
It has to be underlined that in the case of the model of Shin and LaFave (2004), a lower value of τ_4 is assumed in order to use similar values of this shear stress in all the models.

Table 4. Maximum shear stresses (values obtained by assuming f_c=14MPa) of the τ–γ multilinear law.

Model	τ_{max} **[MPa]**
Kim & LaFave (2008)	2.58
Vollum & Newman (1999)	3.29
Ortiz (1993)	3.14
Hwang & Lee (1999)	3.49
Jeon (2013)	2.98

Table 5. Shear stress values of the τ–γ multilinear law

Model		τ_1	τ_2	τ_4
De Risi et al. (2016)	A	1.52	0.85 τ_{max}	0.43 τ_{max}
Celik & Ellingwood (2008)	B1	1.52	0.75τ_{max}	0.16 τ_{max}
	B2	1.52	0.75 τ_{max}	0.30 τ_{max}
Shin & LaFave (2004)	C1	1.52	0.90 τ_{max}	0.30 τ_{max}
	C2	1.52	0.90 τ_{max}	0.30 τ_{max}
Sharma et al. (2011)	D	1.52	0.90 τ_{max}	0.24 τ_{max}

Table 6. Shear strain values of the τ–γ multilinear law.

Model		γ_1	γ_2	γ_3	γ_4
De Risi et al. (2016)	A	0.0004	0.0017	0.0049	0.0441
Celik & Ellingwood (2008)	B1	0.0001	0.002	0.01	0.03
	B2	0.0013	0.01	0.03	0.1
Shin and & LaFave (2004)	C1	0.0005	0.002	0.01	0.03
	C2	0.0005	0.01	0.03	0.05
Sharma et al. (2011)	D	0.0006	0.002	0.005	0.025

4.2 Model calibration and cyclic analyses

In order to identify which of the multilinear τ–γ law obtained by combining the literature models (Table 3) better approximate the monotonic behavior of the joint *J05*, a first set of nonlinear static analyses is carried out. To this purpose, the numerical results in terms of Force-Displacement curves are compared with the envelope curves of the experimental hysteretic cycles.
These preliminary analyses showed that the best approximation of the monotonic response of the specimen is provided by two literature models combinations (see Figure 8 and Figure 9): the first one (*5-A*), obtained by combining the model of Jeon (2013) with the model of De Risi et al. (2016); the second one (*5-C1*), obtained by combining the model of Jeon (2013) with the model of Shin and LaFave (2004).
Then, considering the τ–γ laws derived from the combinations *5-A* and *5-C1*, cyclic analyses are performed in order to calibrate the additional parameters of the *pinching4* material model, specifically from which the loading and unloading branches depend on: the parameter g_F responsible for the strength degradation; the parameters g_K and g_D influencing the unloading and reloading stiffness; the parameters *rDisp*, *rForce* and *uForce* affecting the pinching phenomenon.

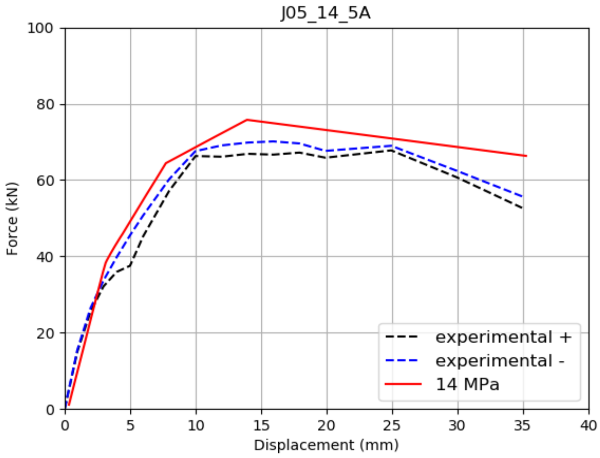

Figure 8. Force-Displacement curves derived from monotonic analyses: *model 5-A*.

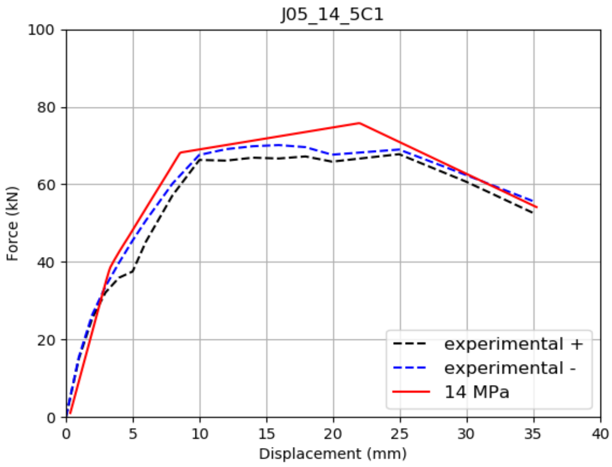

Figure 9. Force-Displacement curves derived from monotonic analyses: *model 5-C1*

To this purpose, an optimization procedure is carried out considering the difference between the numerical and the experimental response in terms of the cumulative dissipated energy *E* and the degradation of the stiffness *K* at every cycle.
In particular, the stiffness K_i at the i-th cycle is assessed through the following formula (Mayes and Clough 1975):

$$K_i = \frac{|F^{+}_{max,i}| + |F^{-}_{max,i}|}{|D^{+}_{max,i}| + |D^{-}_{max,i}|} \tag{8}$$

where $F^{+}_{max,i}$ and $F^{-}_{max,i}$ are the peak lateral forces applied to the beam in the two directions of loading, and $D^{+}_{max,i}$ and $D^{-}_{max,i}$ are the corresponding displacements.

The obtained values of the *pinching4* material parameters which better approximate the cumulative energy dissipation and the stiffness degradation are summarized in Table 7.

Table 7. Calibrated values of the *pinching4* parameters.

	Model 5-A	Model 5-C1
rDisp	0.10	0.10
rForce	0.15	0.15
uForce	-0.40	-0.40
g_{K1}	0.85	0.85
g_{K3}	0.12	0.12
g_{Klim}	0.90	0.85
g_{D1}	0.10	0.10
g_{D3}	0.10	0.10
g_{Dlim}	0.13	0.13

$g_{F1}=g_{F2}=g_{F3}=g_{Flim}=0$; $g_{K2}=g_{K4}=0$; $g_{D2}=g_{D4}=0$.

The good agreement between the experimental results and those obtained by the numerical simulations is shown in Figures 10 and 11 in terms of cumulative dissipated energy, and in Figures 12 and 13 for the stiffness degradation.
From the figures it emerges that the *model 5-A* fits the experimental cumulative energy dissipation better than the *model 5-C1*, whereas no noticeable difference between the two models is observed in terms of stiffness degradation.

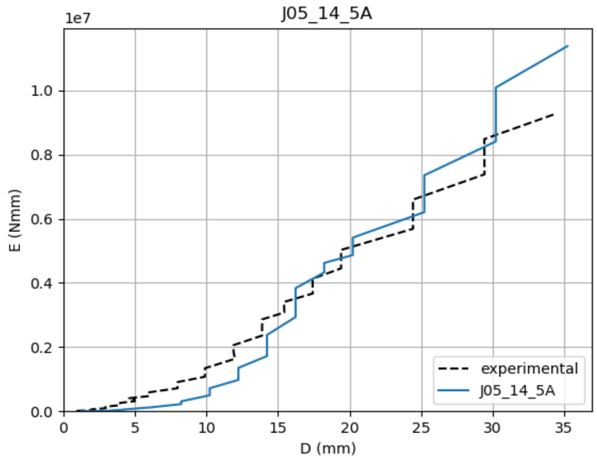

Figure 10. Cumulative dissipated energy for *model 5-A*.

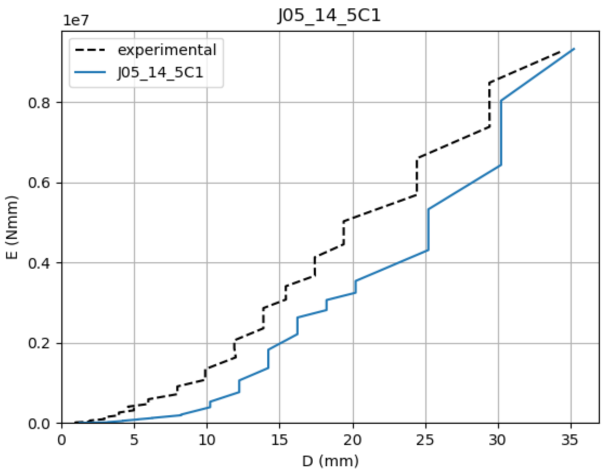

Figure 11. Cumulative dissipated energy for *model 5-C1*.

In Figure 14 and 15 the numerical force-displacement curves, obtained by introducing the parameters of Table 7 in the models *5-A* and *5-C1*, are compared with the experimental ones.
From these figures, it emerges that both the models provide a good approximation of the experimental response of the joint *J05*.
In particular, the model *5-A* is characterized by Force-Displacement cycles very close to the ones emerged from the experimental tests.

4.3 *The role of the concrete strength*

One of the parameters mainly influencing the performance of the beam-column joints is the concrete strength.
As aforementioned, the RC joints analyzed in this paper were built with the aim of reproducing typical joints of existing buildings, which are often characterized by low values of the concrete compressive strength.
For this reason, the “target” compression strength was 16 MPa, but due to issues raised during specimens’ manufacturing, the actual concrete strengths showed a larger scatter around the average value which was about 14 MPa (strengths in the range 10-20 MPa).

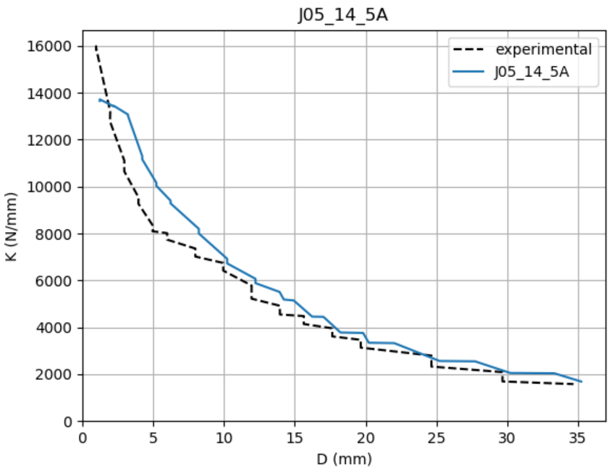

Figure 12. Stiffness degradation for *model 5-A*.

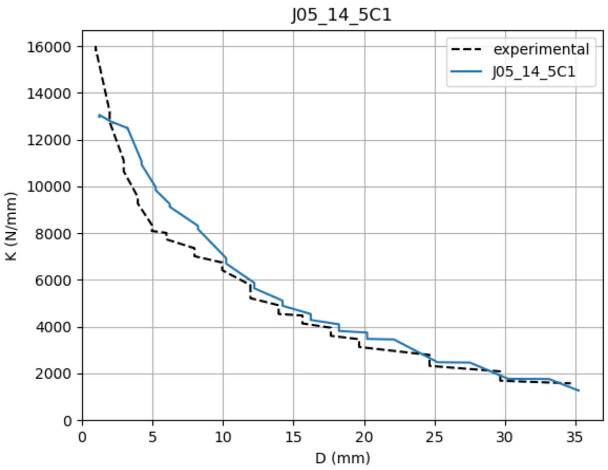

Figure 13. Stiffness degradation for *model 5-C1*.

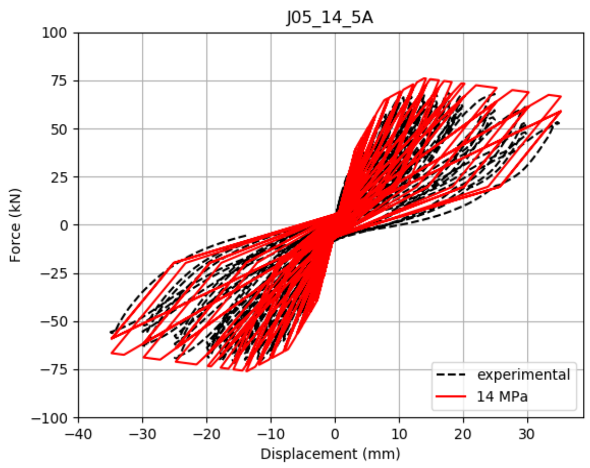

Figure 14. Cyclic response for *model 5-A*.

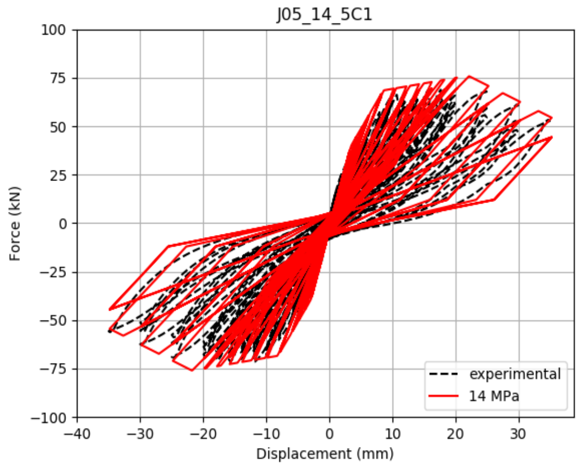

Figure 15. Cyclic response for *model 5-C1*.

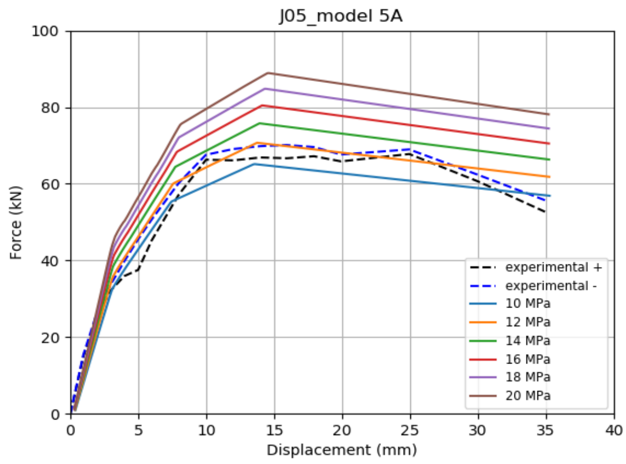

Figure 16. Force-Displacement curves obtained considering different values of the compressive strength of concrete: *model 5-A*.

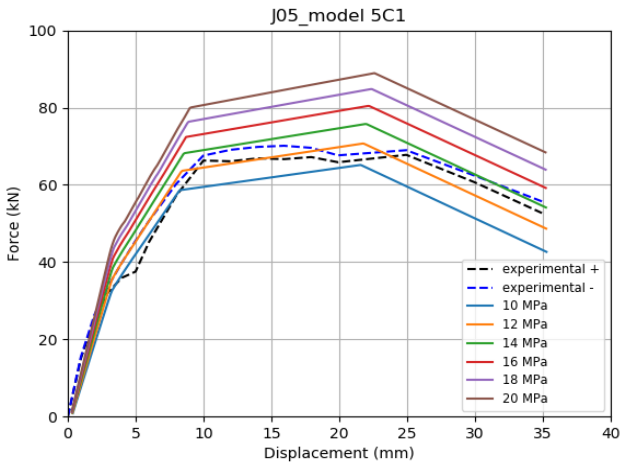

Figure 17. Force-Displacement curves obtained considering different values of the compressive strength of concrete: *model 5-C1*.

Then, in order to investigate the influence of the concrete compressive strength on the reliability of the literature models here analyzed, additional numerical analyses were carried out with reference to the models *5-A* and *5-C1*, by varying the concrete compressive strength from 10 to 20 MPa.

The results obtained from the numerical analyses are reported in Figure 16 and Figure 17 in terms of Force-Displacement curves of the monotonic response.

As expected, the increase of the concrete compressive strength implies a consequent increase of the global strength of the joint.

The cumulative dissipated energy and the stiffness degradation of the cyclic response of the joint are shown in Figures from 18 to 21.

For both the models *5-A* and *5-C1*, the curves that well reproduce the experimental envelopes are the ones corresponding to concrete compressive strength values ranging between 12 and 14 MPa (Figure 16 and Figure 17).

These outcomes highlight the reliability of the proposed models, considering the fact that the experimental activity aimed at analyzing the behavior of beam-column joints characterized by low compressive strength materials.

5 REMARKS AND CONCLUSIONS

The paper has presented the numerical results of nonlinear static and cyclic analyses performed to simulate the behavior of exterior reinforced concrete beam–column joints, without transverse beams, tested at the University of Salerno.

In particular, the numerical analyses have been carried out by considering some theoretical models available in literature which were calibrated by the authors on the base of the experimental results.

The main considerations emerging from the analyses are summarized in the following.

The monotonic numerical response of the joint *J05* is better simulated by two sets of literature models: the first is given by combining the model of Jeon (2013) with the model of De Risi et al. (2016); the second one by combining the model of Jeon (2013) with the model of Shin and LaFave (2004).

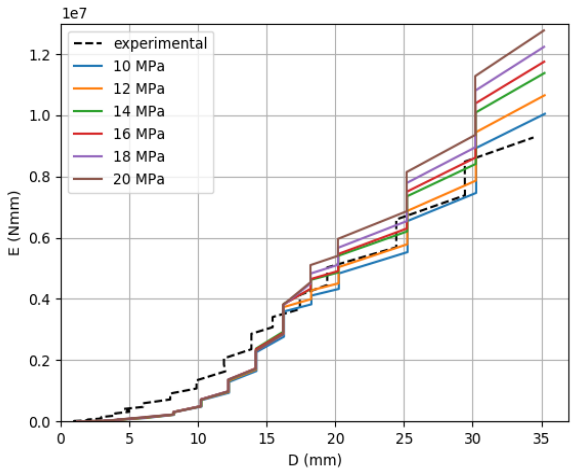

Figure 18. Cumulative dissipated energy in the case of different concrete strengths: *model 5-A*.

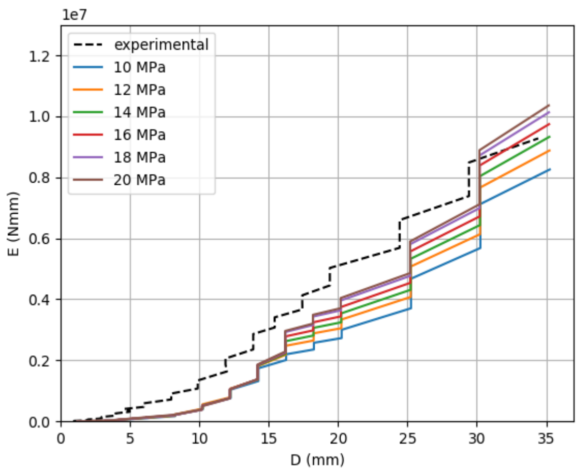

Figure 19. Cumulative dissipated energy in the case of different concrete strengths: *model 5-C1*.

The same sets of models also provide a good prediction of the envelop curves of the experimental cyclic responses.

The evaluation of the cyclic behavior of the joint requires a proper procedure for setting the parameters controlling the unloading and reloading laws (to reproduce both strength and stiffness degradation) and the pinching phenomenon.

The calibration of such parameters strongly depends on the reference analytical model, i.e. on the definition of a backbone curve. This consideration was confirmed by the outcomes of this study.

The obtained results and the corresponding observations are very important for the development of reliable models of strengthened joints. Of course, further research is needed in order to better understand the reliability of the analytical models in representing the seismic response of the beam-column joint elements. This is even more important in the simulation of the cyclic behavior, where the degradation in terms of stiffness and strength is the main feature affecting the outcomes.

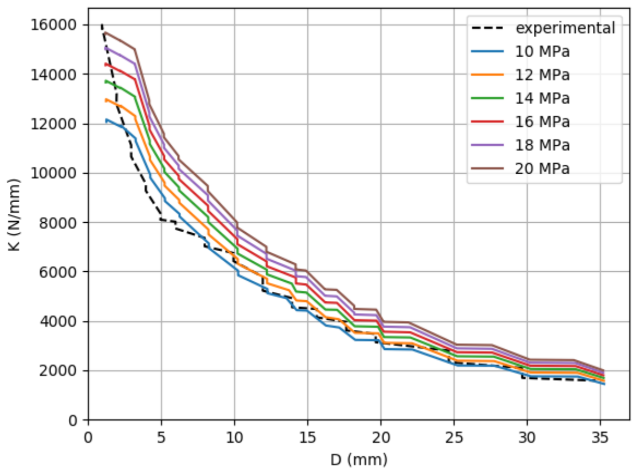

Figure 20. Stiffness degradation in the case of different concrete strengths: *model 5-A*.

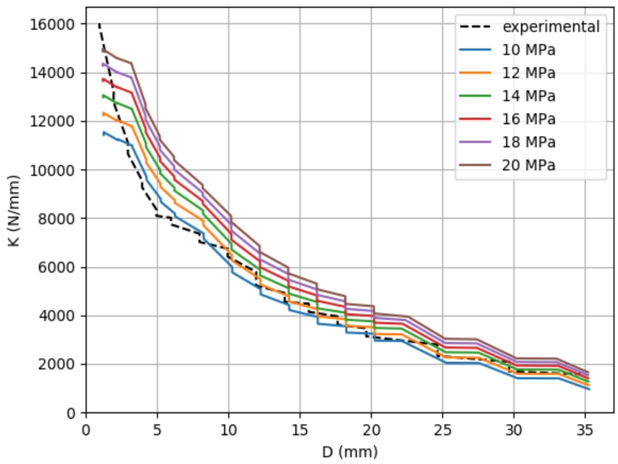

Figure 21. Stiffness degradation in the case of different

Finally, the performed parametric analyses confirmed that cyclic behaviour of beam-column joints is significantly influenced by the compressive strength of concrete.

6 ACKNOWLEDGEMENTS

This work was performed in the framework of the project "DPC/ReLUIS 2019-2021" (WP2 & WP14).

7 REFERENCES

Akguzel, U., Pampanin, S., 2012. Assessment and design procedure for the seismic retrofit of reinforced concrete beam-column joints using FRP composite materials, *Journal of Composites for Construction*, **16**(1), February 1, 2012.

Alath, S., Kunnath, SK., 1995. Modeling inelastic shear deformations in RC beam–column joints, *Engineering mechanics proceedings of 10th conference*. ASCE, New York, **2**, 822-5. May 21-24, University of Colorado at Boulder, Boulder, Colorado.

Altoontash, A., 2004. Simulation and damage models for performance assessment of reinforced concrete beam-column joints. *Ph.D. Thesis*, Department of Civil and Environmental Engineering, Stanford University, USA.

Biddah, A., Ghobarah, A., 1999. Modelling of shear deformation and bond slip in reinforced concrete joints, *Structural Engineering,* **7**(4), 413-32.

Celik, OC., Ellingwood, BR., 2008. Modeling Beam Column Joints in Fragility Assessment of Gravity Load Designed Reinforced Concrete Frames, *Journal of Earthquake Engineering,* **12**, 357-381.

Decreto ministeriale 14 gennaio 2008, NTC 2008. Norme tecniche per le costruzioni, *G.U. n.29 del 4 febbraio 2008.*

Decreto ministeriale 17 gennaio 2018, NTC 2018. Aggiornamento delle "Norme tecniche per le costruzioni", *G.U. n.42 del 20 febbraio 2018.*

Del Vecchio C., Di Ludovico M., Balsamo A., Prota A., Manfredi G., Dolce M., 2014. Experimental investigation of exterior RC beam-column joints retrofitted with FRP systems, *Journal of Composites for Construction.* August, 2014.

De Risi, MT., Ricci, P., Verderame, GM., Manfredi, G., 2015. A nonlinear macro model for numerical simulation of exterior RC joints without transverse reinforcement, *Second European Conference on Earthquake Engineering and Seismology.* August 25-29, 2014, Istanbul, Turkey.

De Risi, MT., Ricci, P., Verderame, GM., 2016. Modelling exterior unreinforced beam-column joints in seismic analysis of non-ductile RC frames, *Earthquake Engineering & Structural Dynamics.* November, 2016.

De Vita, A., Faella, C., Napoli, A., Realfonzo, R., 2017. Cyclic response of R/C Beam-Column Joints Strengthened with Steel FRP/FRCM Composite Materials, *In Proceedings of the XVII Anidis Congress "L'Ingegneria Sismica in Italia".* September 17-21, Pistoia, Italy.

Hwang, S., Lee, H., 1999. Analytical model for predicting shear strengths of exterior reinforced concrete beam-column joints for seismic resistance, *ACI Structural Journal,* **96**(5), 846-857.

Jeon, JS., 2013. Aftershock vulnerability assessment of damaged reinforced concrete buildings in California. *Ph.D. Thesis,* School of Civil and Environmental Engineering, Georgia Institute of Technology, GA, USA.

Jeon, JS., Lowes, LN.,DesRoches, R., Brilakis, I., 2015. Fragility curves for non-ductile reinforced concrete frames that exhibit different component response mechanisms, *Engineering Structures,* **85**, 127-143.

Kim, J., LaFave, J.M., 2008. Joint shear behavior prediction in RC beam-column connections subjected to seismic lateral loading, *In: The 14th World Conference on Earthquake Engineering.* October 12-17, Beijing, China.

Lowes, LN., Altoontash, A., 2003. Modeling Reinforced-Concrete Beam-Column Joints Subjected to Cyclic Loading, *Journal of Structural Engineering.* **129**, 1686-1697.

Mayes, RL., Clough, RW., 1975. State of the art in seismic shear strength of masonry – An evaluation and review, *EERC Report.* Berkeley, California, USA.

McKenna, F., Fenves, GL., Scott, MH., 2010. OpenSees: Open System for Earthquake Engineering Simulation, Pacific Earthquake Engineering Research Center. University of California, Berkeley, CA, USA. http://opensees.berkeley.edu, 2010.

Milanese, G., 2017. Valutazione dell'efficacia di sistemi di rinforzo SRP e SRG per ilrinforzo strutturale dei nodi trave-pilastro in C.A, *M.Sc. Thesis,* Department of Civil Engineering, University of Salerno, Italy.

Mitra, N., Lowes, LN., 2007. Evaluation, calibration, verification of a reinforced concrete beam-column joint model, *ASCE Journal of Structural Engineering,* **133**(1), 105-120.

Napoli, A., Faella, C., Perri, F., Realfonzo, R., 2016. Strengthening of RC beam-column joints with SRP/SRG systems, *The New Boundaries of Structural Concrete, Workshop Proceedings.* Capri, Italy.

Ortiz, IR., 1993. Strut-and-Tie Modeling of Reinforced Concrete Short Beams and Beam-Column Joints, *Ph.D. Thesis,* University of Westminster. London, United Kingdom.

Realfonzo R., Napoli, A., Ruiz Pinilla, JG., 2014. Cyclic behavior of RC beam-column joints strengthened with FRP systems, *Construction and Building Materials,* **54**, 282-297.

Shafaei, J., Zareian, S., Hosseini, A., Marefat, MS., 2013. Effect of joint flexibility on the overall performance of reinforced concrete structure, *The Fourth International Conference on Concrete and Development.* April 29-May 1, Tehran, Iran.

Sharma, A., Eligehausen, R., Reddy, GR., 2011. A new model to simulate joint shear behavior of poorly detailed beam–column connections in RC structures under seismic loads, part I: exterior joints, *Engineering Structures,* **33**(3), 1034-1051.

Shin, M., LaFave, J.M., 2004. Testing and modelling for cyclic joint shear deformations in RC beam–column connections**,** *Proceedings of the thirteenth world conference on earthquake engineering,* August 1-6, Vancouver, B.C., Canada.

Uzumeri, SM., 1977. Strength and ductility of cast-in-place beam-column joints, *American Concrete Institute Annual Convention, Symposium on Reinforced Concrete Structures in Seismic Zones,* **53**, 293-350. San Francisco, 1974.

Vecchio, FJ., Collins, MP., 1986. The modified-compression fiel theory for reinforced concrete elements subjected to shear, *ACI Journal, Proceedings,* **83**(2), 219-231.

Vollum, RL., Newman, JB., 1999. Strut and tie models for analysis/design of external beam-column joints, *Magazine of Concrete Research;* **51**(6), 415-425.